Dentomaxillofacial Radiology (2015) 44, 20150098

birpublications.org/dmfr

RESEARCH ARTICLE

Stationary intraoral digital tomosynthesis using a carbon nanotube X-ray source array

[1]J Shan, [2]A W Tucker, [3]L R Gaalaas, [1]G Wu, [3]E Platin, [3]A Mol, [1]J Lu and [1,4]O Zhou

[1]Department of Physics and Astronomy, University of North Carolina at Chapel Hill, Chapel Hill, NC, USA; [2]Xintek Inc., Research Triangle Park, NC, USA; [3]University of North Carolina School of Dentistry, Chapel Hill, NC, USA; [4]Lineberger Comprehensive Cancer Center, University of North Carolina at Chapel Hill, Chapel Hill, NC, USA

Objectives: Intraoral dental tomosynthesis and closely related tuned-aperture CT (TACT) are low-dose three-dimensional (3D) imaging modalities that have shown improved detection of multiple dental diseases. Clinical interest in implementing these technologies waned owing to their time-consuming nature. Recently developed carbon nanotube (CNT) X-ray sources allow rapid multi-image acquisition without mechanical motion, making tomosynthesis a clinically viable technique. The objective of this investigation was to evaluate the feasibility of and produce high-quality images from a digital tomosynthesis system employing CNT X-ray technology.

Methods: A test-bed stationary intraoral tomosynthesis unit was constructed using a CNT X-ray source array and a digital intraoral sensor. The source-to-image distance was modified to make the system comparable in image resolution to current two-dimensional intraoral radiography imaging systems. Anthropomorphic phantoms containing teeth with simulated and real caries lesions were imaged using a dose comparable to D-speed film dose with a rectangular collimation. Images were reconstructed and analysed.

Results: Tomosynthesis images of the phantom and teeth specimen demonstrated perceived image quality equivalent or superior to standard digital images with the added benefit of 3D information. The ability to "scroll" through slices in a buccal–lingual direction significantly improved visualization of anatomical details. In addition, the subjective visibility of dental caries was increased.

Conclusions: Feasibility of the stationary intraoral tomosynthesis is demonstrated. The results show clinical promise and suitability for more robust observer and clinical studies.
Dentomaxillofacial Radiology (2015) **44**, 20150098. doi: 10.1259/dmfr.20150098

Cite this article as: Shan J, Tucker AW, Gaalaas LR, Wu G, Platin E, Mol A, et al. Stationary intraoral digital tomosynthesis using a carbon nanotube X-ray source array. *Dentomaxillofac Radiol* 2015; **44**: 20150098.

Keywords: intraoral X-ray; intraoral tomosynthesis; stationary tomosynthesis; carbon nanotube X-ray source

Introduction

Since Wilhelm Rontgen first discovered X-rays in 1895, dental radiology has experienced several milestones. These include the development of panoramic radiography, dental tomography, dental tomosynthesis, more efficient image detectors, digital radiography and, most recently, CBCT.[1–3] CBCT has found wide acceptance in the dental community because of its ability to provide a three-dimensional (3D) representation of the hard tissues of the oral and maxillofacial region.[3] While CBCT has demonstrated its value for many applications, it has

Correspondence to: Dr Jing Shan. E-mail: jingshan@unc.edu

The authors A W Tucker and J Shan contributed equally to this study.

This research was partially supported by a UNC internal research fund, and research grant R43DE024933 from the National Institute of Dental and Craniofacial Research of National Institute of Health.

Received 17 March 2015; revised 9 June 2015; accepted 17 June 2015

not been conclusively shown to improve caries detection.[3–6] In part, this is as a result of beam-hardening artefacts that occur in teeth and its relatively low-spatial resolution. These artefacts may obscure existing caries lesions or may result in false-positive diagnoses. Even a high-resolution CBCT system with a small field of view has not shown improvement in the detection of proximal caries lesions.[6] The increased financial cost, patient dose and practitioner time associated with using CBCT to diagnose caries are additional disadvantages when compared with conventional two-dimensional (2D) modalities.

The need to reliably detect proximal and occlusal caries using a low-dose, low-cost and time-efficient imaging modality remains a high oral health priority.[7] Caries affects millions of Americans and, when undetected, could evolve into more serious conditions that may require large restorations, endodontic treatment or extractions. Radiology has always played a vital role in caries diagnosis, particularly in areas of the teeth where diagnostic efficacy of the clinical examination is limited. Currently, the most widely used imaging modality for the detection of proximal caries lesions is bitewing radiography.[8] Unfortunately, the diagnostic accuracy of bitewing radiographs for the detection of dental caries is quite low. A systematic review of the literature by Bader et al[8] showed median sensitivity and specificity values for radiographic occlusal caries detection of 27% and 95%, respectively. For proximal caries, the median values were 49% and 88%. The main challenge in occlusal and proximal caries lesions is the need to detect small levels of mineral loss in otherwise highly mineralized tissues of enamel and dentin.[9] The superimposition of these tissues limits subject contrast, as the radiographic appearance of lesions is highly dependent on the projection geometry.[7] Furthermore, incorrect image geometry resulting in "closed contacts" can significantly compromise the visualization of lesions.

In the late 1990s, several studies explored the potential use of dental tomosynthesis for caries detection and a variety of dental conditions. Both conventional digital tomosynthesis and tuned-aperture CT (TACT) were investigated. Conventional digital tomosynthesis moves a single X-ray source in a limited angular path, acquiring images at different locations. Digital sensors, either intraoral or extraoral, are mechanically connected to the rotating tube, fixing the acquisition geometry.[10–13] TACT uses a small number of angular projections as in tomosynthesis, but images are acquired using a single fiduciary marker associated with the irradiated object. The projection of the fiduciary marker allows the projection geometry to be determined post-acquisition without knowing the exact aperture.[14] Several studies have shown the efficacy of TACT for a number of diagnostic tasks, including root fracture detection, the detection and quantification of periodontal bone loss, implant site assessment and the evaluation of impacted third molars.[7,15–22] In addition, some studies have shown that tomosynthesis improved proximal and occlusal caries detection.[7,11,20–22] One observer study[11] showed a sensitivity of 71% and diagnostic accuracy of 81.8%, which are higher than in conventional 2D intraoral radiography. These techniques, both tomosynthesis and TACT for dental applications, have not been implemented clinically, largely owing to the slow procedure needed to change the position of the X-ray source to acquire projection images, slow detector acquisition speed and relatively long reconstruction times at the time of study. With current improvements of digital sensors, computer speed and development of carbon nanotube (CNT) field emission X-ray source arrays, the technique shows more promise for clinical implementation. Currently, tomosynthesis is used for chest,[23–25] abdominal,[26] musculoskeletal[27,28] and breast imaging applications.[23,24,29]

Most recently, researchers at the University of North Carolina, Department of Physics and Astronomy developed a CNT-based field emission X-ray source array technology.[30,31] This innovation addresses many of the shortcomings of previous dental tomosynthesis and TACT imaging techniques. Multiple individually controllable X-ray sources are spatially distributed in a single X-ray tube to eliminate the need to position the X-ray source at different locations during image acquisition. This technology enables stationary tomography, which has been demonstrated in digital breast tomosynthesis,[32–34] digital chest tomosynthesis,[35,36] tomosynthesis-guided radiation therapy[37] and stationary CT for homeland security.[38] The purpose of this study was to investigate the feasibility of using a CNT X-ray source array for stationary intraoral tomosynthesis (s-IOT).

Methods and materials

System description

A test-bed stationary tomosynthesis system, as shown in Figure 1a, was modified to investigate the feasibility of s-IOT. The system included a CNT source array (model 2008-08-L75-002; XinRay Systems Inc., Research Triangle Park, NC), an intraoral digital sensor (SuniRay2; Suni Medical Imaging Inc., San Jose, CA) and control electronics. The source array was operated at 70 kVp, which is commonly used for intraoral radiography applications.[10,39] The SuniRay2 intraoral sensor is a standard size #2 sensor with a field of view of 35.2 × 25.2 mm and a pixel size of 33 × 33 μm. The detector begins integration right after exposure to X-rays and reads out images when the X-ray source is turned off. Customized software was developed to automate the continuous projection image acquisition. The X-ray output was controlled by a multipixel switching electronics from XinRay Systems. As illustrated in the timing diagram in Figure 2, the CNT source array was fired following a trigger sequence initiated by the operator, the X-ray pulse triggered the digital sensor and the projection image was acquired and saved.

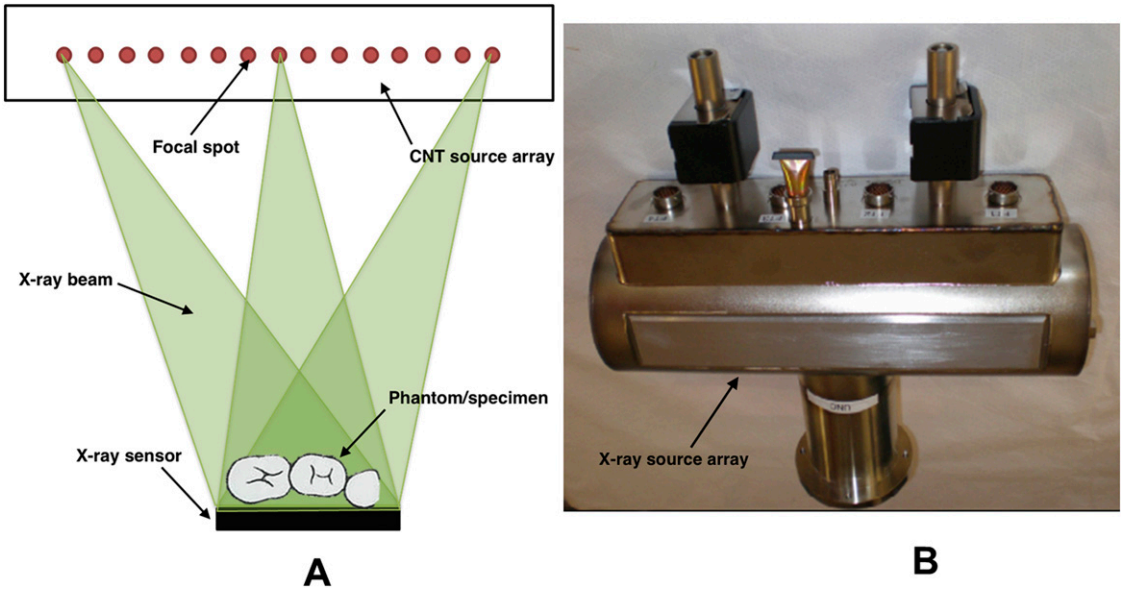

Figure 1 (a) Illustration of the stationary intraoral tomosynthesis system set-up. The system consists of a carbon nanotube (CNT) X-ray source array and intraoral sensor. Projection images are acquired by electronically switching individual focal spot inside the source array. (b) Photo of the source array. CNT X-ray sources are linearly distributed in the linear source array.

Distributed carbon nanotube X-ray source array

The CNT source array used for this study was not designed specifically for dental image applications. It had 75 linearly distributed X-ray focal spots with a 4-mm pitch. Each individual source inside the source array consisted of a CNT cathode, gate and focusing electrodes and a shared elongated tungsten anode. The picture of CNT X-ray source is shown in Figure 1b. A 2-mm aluminium window served as both the vacuum barrel and the inherent filtration, resulting in a half-value layer of 2 mm aluminium, which complies with the Food and Drug Administration regulations that apply to X-ray beam quality for dental applications.[40] The CNT cathode emits electrons using the field emission effect.[31,41] The emission current is solely controlled by the electric field applied between the CNT cathode and gate electrode. The maximum output current as in conventional X-ray sources is limited by thermal management of the anode and is determined by many factors such as focal spot size, anode voltage and X-ray pulse width.[42] The average focal spot size was measured as 2.5×0.5 mm (full width at half maximum) with the elongated direction along the source array.[36] The tube was operated at 5-mA tube current comparable to conventional intraoral X-ray sources.[10,11,39] A subset of the 75 sources was used for this study.

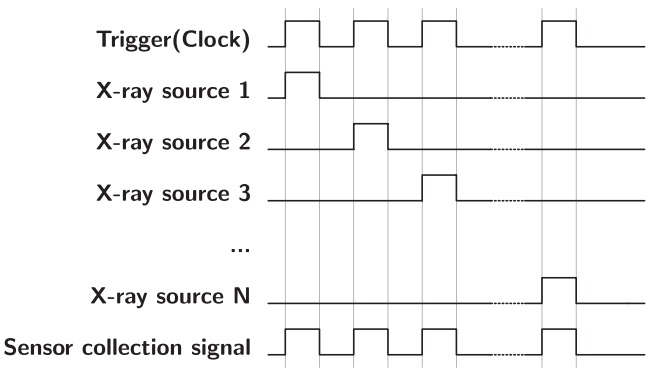

Figure 2 Timing diagram of the stationary intraoral tomosynthesis system. The source array was triggered by an external trigger signal. Individual X-ray sources were fired in a sequence set by the operator. The sensor was triggered by X-ray pulses to collect and save a set of projection images.

System parameters and imaging protocol

One of the aims of this study was to investigate the feasibility of acquiring bitewing tomosynthesis images with the accumulated radiation dose comparable to a conventional 2D intraoral bitewing image. The standard bitewing technique used at the University of North Carolina School of Dentistry's radiology clinic was used as a reference. The technique used a photostimulable phosphor intraoral receptor with a Focus™ Instrumentarium intraoral source (Instrumentarium Dental, Tuusula, Finland) operating at 70 kVp, 7 mA, 0.32 s, 40 cm source-to-image distance (SID) and a standard 30-cm rectangular collimation.

The focal spot size of this CNT source array is significantly larger than those used in conventional intraoral X-ray systems. In order to compensate for the loss in resolution owing to focal spot size, the source was positioned at 840 mm from the detector. This distance was determined by simulating the modulation transfer function (MTF) that characterizes the spatial resolution of the projection images, adapted from a method described by Marshall and Bosmans.[43] At this

distance, the image spatial resolution was equivalent to the resolution commonly used in conventional intraoral radiography.

To match the radiation dose of the s-IOT to the clinical 2D intraoral radiography, the X-ray output was measured using a calibrated Unfors Mult-O-Meter 470L solid-state dosimeter (Unfors Instruments AB, Billdal, Sweden). The dosimeter probe was aligned to the X-ray source array and placed at a distance of 100 cm from the focal spot. The incident air kerma was measured at 70 kVp and various mAs values from 0.3 mAs (5 mA × 60 ms) to 0.8 mAs (5 mA × 160 ms). Multiple dose measurements were performed at each tube output. The tube output (measured in mAs) per projection image was calculated based on measured dose of the source array and clinical 2D intraoral radiography technique scaled by SID.

Reconstruction

Projection images were reconstructed using the adaptive fan-beam volume reconstruction algorithm with a simultaneous algebraic reconstruction technique (SART).[44] Reconstruction of the 3D data set was broken down into a series of 2D slice reconstructions. This approach was taken to increase reconstruction speed and reduce memory usage. Raw images were preprocessed so that the X-ray source array was perfectly aligned with the detector row and were scaled so that the same system matrix could be applied to every reconstructed 2D slice. For each 2D reconstruction, total variation (TV) regularization was applied to reduce artefacts and improve overall image quality. The unknown parameter Nesterov algorithm was used to minimize the TV without enforcing the strong convexity property.[45] All images were reconstructed on a customized workstation with one Intel® Core™ i7-5930K processor (six cores, 3.5 GHz; Intel Corporation, Santa Clara, CA).

Phantom and specimen images

An anthropomorphic dental quality assurance phantom (RMI model 501A; Radiation Measurements Inc., Middleton, WI) was imaged by the s-IOT system. The phantom is designed to simulate common clinical intraoral imaging tasks. A portion of maxillary alveolar bone and teeth with simulated caries lesions and metallic restorations are embedded in the phantom. For direct comparison, the phantom was also imaged with a 2D intraoral system (Focus™ X-ray; Instrumentarium Dental) at the University of North Carolina (UNC) School of Dentistry. The SuniRay2 intraoral digital sensor was used to acquire images for both the s-IOT system and the 2D radiography system. Both modalities used a tube voltage of 70 kVp. The same imaging dose was used for the 2D intraoral image sets and tomosynthesis data sets. The phantom was placed on the detector housing in order to better represent an intraoral design. In addition, a phantom constructed using three extracted teeth specimen with real caries lesions obtained from the UNC School of Dentistry teaching materials was also imaged. The teeth were mounted on cadaver material and covered with approximately 1 cm of wax to simulate the effects of soft-tissue attenuation. The phantom was imaged with both the s-IOT system and the 2D radiography systems for comparison. Caries ground truth status was established by micro-CT (μCT).[46,47] The μCT scans were acquired with a Scanco Medical μCT 40 scanner (Scanco Medical AG, Bruttisellen, Switzerland) operating at 70 kVp, 0.115 mA, 200 s scan time, with 0.5 mm aluminium filtration. Scans were reconstructed with a 20-μm voxel size using Scanco v. 1.2a software (Scanco Medical AG). μCT scans were reviewed by a trained dental radiologist (LG) to confirm caries lesion status.

Results

System characterizations

Figure 3 plots the relationship between the incident air kerma and the tube output in phototimed mAs at 100 cm from the focal spots at 70 kVp. The incident air kerma per mAs was 63.69 μGy mAs^{-1}. A larger SID was used in the imaging set-up to remedy the loss of image resolution owing to the large focal spot size. At the adjusted 840-mm SID, the MTFs of the system that characterize the image resolution are simulated and plotted in Figure 4. The MTF curve of the s-IOT (blue curve; for colour image see online) using adjusted imaging parameters (840-mm SID) is compared with the standard 2D intraoral system (1.1-mm focal spot size, 370-mm SID). 10% of MTF yields a spatial resolution of 10.05 cycles mm^{-1} for the s-IOT system, which is similar to the 10.47 cycles mm^{-1} of the aforementioned 2D intraoral system at the UNC School of Dentistry.

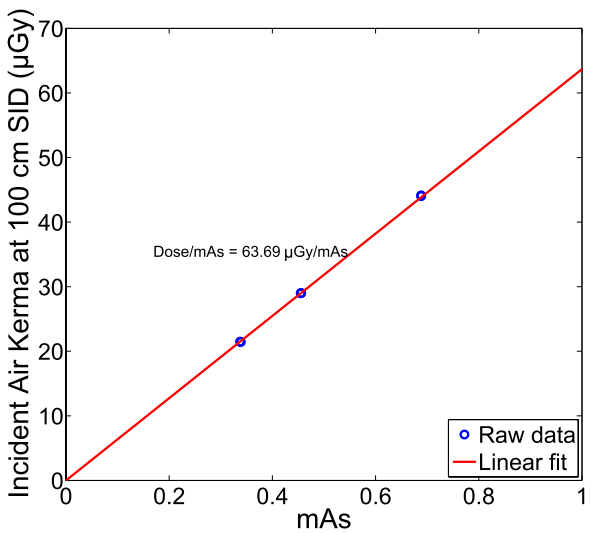

Figure 3 Relationship between incident air kerma at 100 cm from focal spot and the X-ray tube output (mAs). The air kerma is linear to the anode output. The incident air kerma per mAs at 100 cm was 63.69 μGy mAs^{-1}. SID, source-to-image distance.

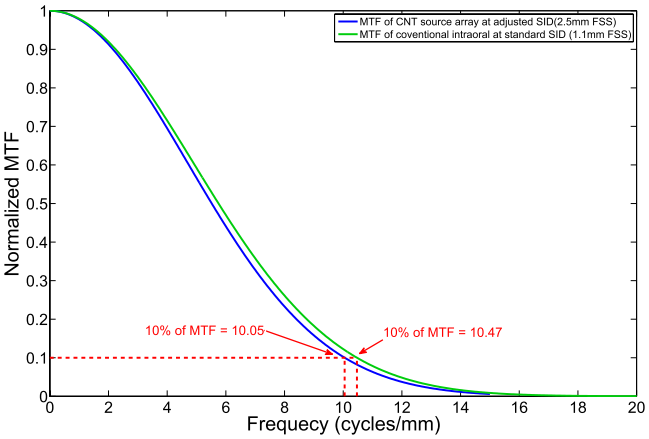

Figure 4 Simulated modulation transfer function (MTF) of the stationary intraoral tomosynthesis (s-IOT) system. The blue curve simulates the MTF of s-IOT at the adjusted source-to-image distance (SID), while the green curve is the simulated MTF of the standard 2D intraoral system [1.1-mm focal spot size (FSS), 33-μm detector pixel size and 370-mm SID]. The spatial resolution of the s-IOT was 10.05 cycles mm^{-1} with the adjusted system parameters, which is comparable to commercial 2D intraoral radiography systems. CNT, carbon nanotube. For colour images see online.

The spatial resolution of s-IOT was also comparable to the image resolution of 7–20 cycles mm^{-1} of commercial intraoral radiography systems reported in literatures.[48,49] Based on the system characterizations and the reference 2D intraoral radiography technique, the tube output per projection was calculated.

Figure 5 shows the waveforms of anode current captured by an oscilloscope for all the sources in the source array. All sources using 5-mA anode current show a consistent output from source to source with very fast switching (on/off speed).

Phantom imaging

Projection images of the anthropomorphic phantoms were acquired and reconstructed for quality assessment. The 2D X-ray image and the selected reconstructed tomosynthesis slices of the RMI phantom are shown in Figure 6. The tomosynthesis image sets were reconstructed using 15 projections acquired over a 12.7° angular span at a SID of 840 mm. The number of projections and angular coverage are comparable to the imaging parameters used in previous dental tomosynthesis studies.[10,11] The mAs per projection image was 1.05 mAs (5 mA × 210 ms) for a total exposure of 15.75 mAs. This accumulated radiation dose for the entire tomosynthesis scan is approximately equal to the dose of a single 2D intraoral image using D-speed film with rectangular collimation. This dose is at the same level of intraoral imaging systems used in dental clinics today.[50] Images were reconstructed using the SART. Reconstructed images were examined by experienced dental radiologists, and it was determined that reconstruction with 20 iterations was most preferred. This provided details and overall smoothness with low noise level and good sharpness. Dental tomosynthesis reconstruction using SART was completed in 8 s. The application of TV regularization resulted in a reconstruction time of 90 s.

Figure 6a shows a photograph of the RMI dental phantom of a partial jaw with teeth with simulated lesions and metal fillings. Figure 6b shows the standard 2D intraoral image of the phantom. Figure 6c–f shows the selected tomosynthesis slices focused at the buccal molar roots, palatal molar root, simulated caries defects and tooth fractures, respectively. Compared with conventional 2D intraoral image, the tomosynthesis image of the RMI phantom shows increased visualization of dental anatomy, simulated lesions and tooth fractures. Based on the images of metal restorations in the RMI phantom, the reconstructed images also demonstrate subjectively minor beam-hardening and streak artefacts.

Figure 7 shows the comparison between the 2D intraoral image and the tomosynthesis slices for a phantom constructed using extracted teeth, with μCT images of the teeth as ground truth to validate the lesion. Figure 7a shows the standard 2D intraoral radiograph, while Figure 7b–d shows the selected tomosynthesis slices focusing at different depth. The μCT images of the three teeth are shown in Figure 7e–g as ground truth to validate the lesions. The reconstructed images of the extracted teeth demonstrate subjectively better lesion contrast and definition than standard 2D intraoral images. The tomosynthesis slices also provide better localization of the lesion in the buccal–lingual direction.

Discussions

In this study, a proof-of-concept s-IOT was demonstrated. The reconstructed tomosynthesis slices of an anthropomorphic phantom and extracted teeth have

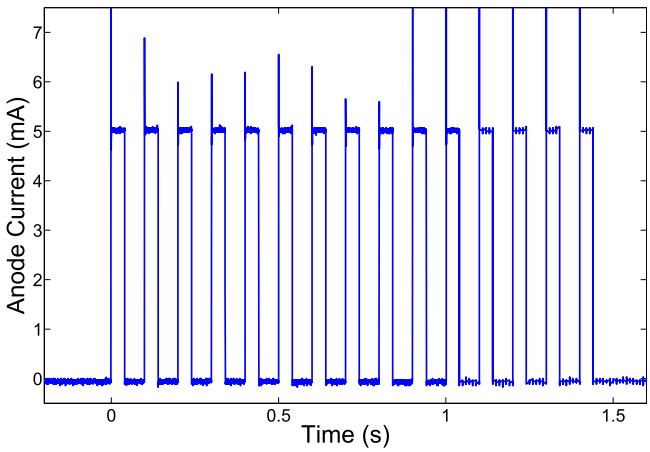

Figure 5 The anode current waveform for 5 mA and 40-ms pulse width from all 15 sources. The waveform shows consistent current output from source to source. The overshoot signal at the beginning of each pulse was the step response of the switching electronics, which was not a real anode current overshoot.

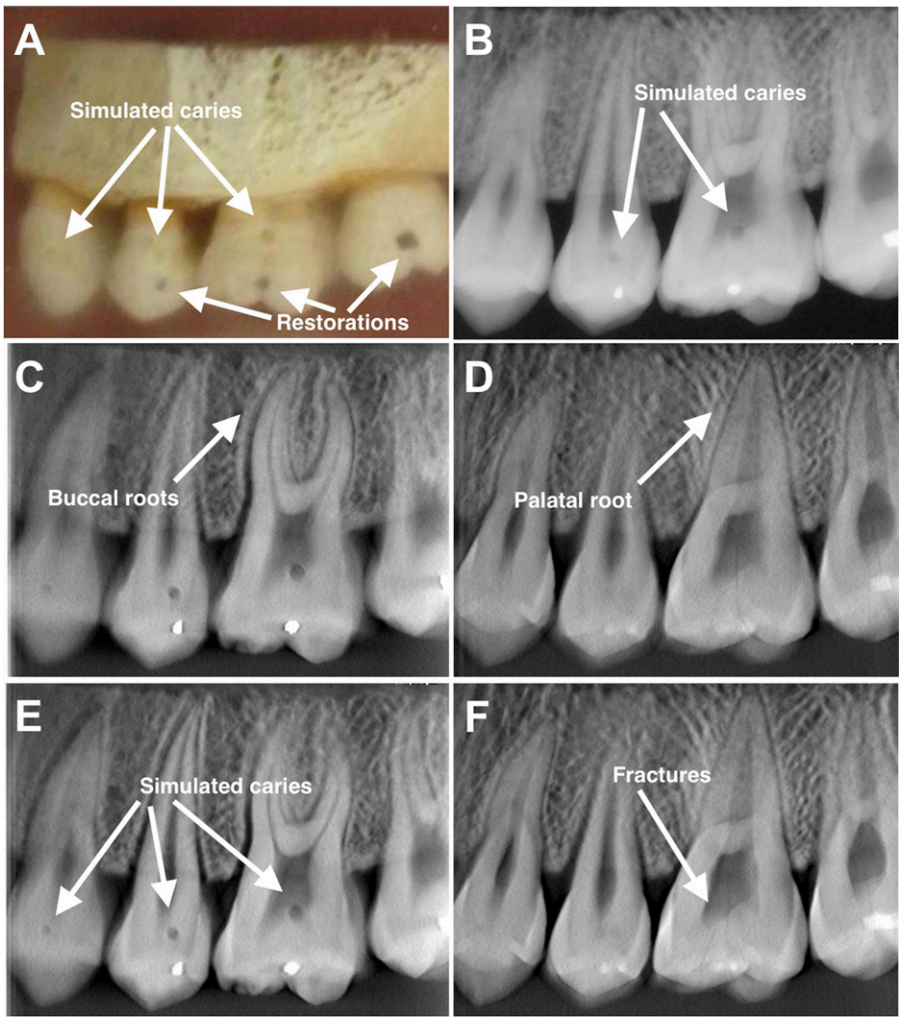

Figure 6 Comparison between two-dimensional (2D) intraoral radiography and stationary intraoral tomosynthesis (s-IOT). (a) The photograph of the RMI dental phantom (RMI model 501A; Radiation Measurements Inc., Middleton, WI). (b) A standard 2D radiograph. (c–f) The selected tomosynthesis slices focus at different planes. (c) The details in buccal molar roots. (d) The palatal molar root. (e) The simulated buccal defects. (f) The tooth fractures.

shown improved subjective visibility and detection of dental pathology such as caries, root fractures and alveolar defects compared with 2D intraoral radiography. Tomosynthesis slices are reconstructed using low-dose projection images acquired at various positions, avoiding image angulation errors that cause "closed contacts" in standard 2D intraoral radiography. Tomosynthesis images also revealed high-detail 3D information of dental and alveolar anatomy using a dose equal to conventional intraoral images and with less metal streak artefacts than CBCT. The efficacy of this modality will be further examined with observer and clinical studies. A reader study evaluating the detection of caries using extracted teeth has been approved by the institutional review board at UNC and is currently under way. The results will be reported in the near future.

Compared with previous studies, this study addressed some of the issues associated with conventional dental tomosynthesis and TACT, which may enable clinical implementation of the technology in future. The s-IOT acquires projection images by electronically firing each individual X-ray source inside the source array without mechanically moving it. The reconstruction time is as short as 8 s using the SART algorithm without graphics processing unit acceleration.

The main parameters affecting tomosynthesis image quality are tomosynthesis angular coverage and the number of projections. An angular coverage of 12.7° was used in the s-IOT systems, which is comparable to previous studies.[10,11] Larger angular coverage leads to better in-depth resolution.[34,51,52] However, owing to the size limit of intraoral digital sensors, a larger tomosynthesis angular coverage will result in a smaller field of view limiting the clinical usefulness of the technology. The flexibility of the CNT source array also allows a non-linear-shaped source array that may improve the image quality.[53] The optimized source array design and imaging configurations are currently being investigated.

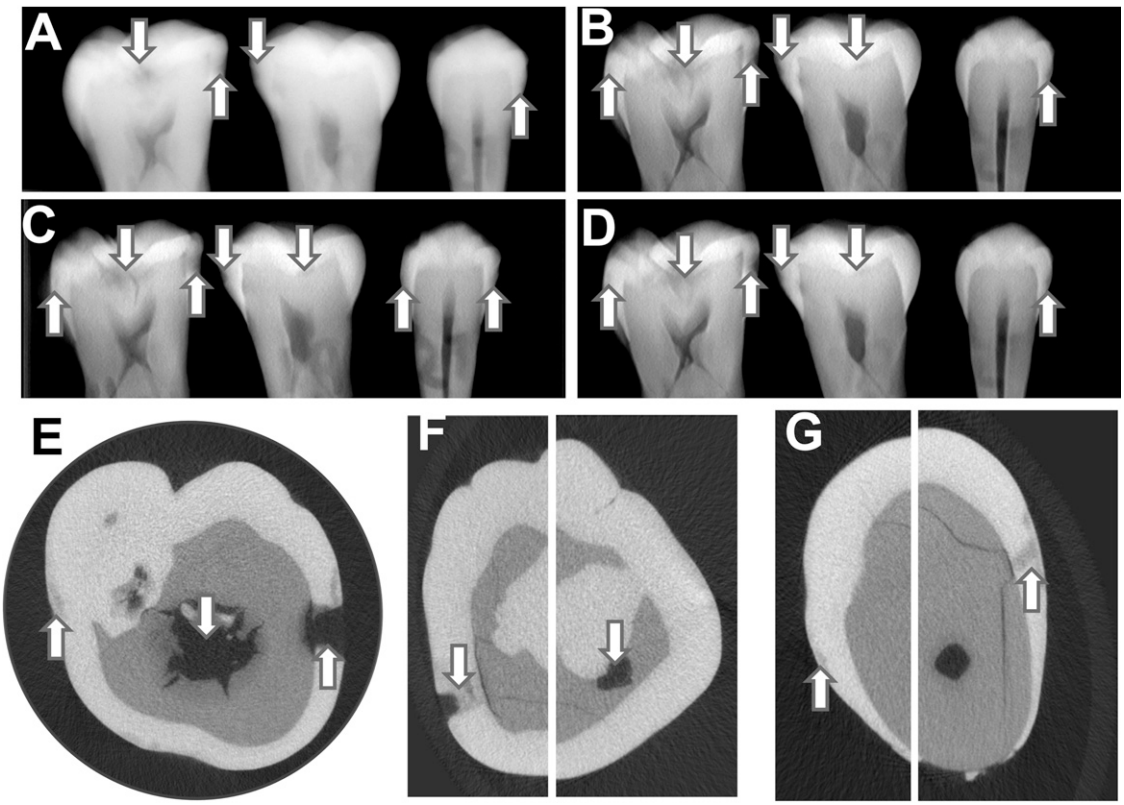

Figure 7 Comparison between the standard two-dimensional (2D) radiograph (a) and stationary intraoral tomosynthesis (s-IOT) slices (b–d) of the extracted teeth with axial micro-CT ground truth images (e–g). Arrows on the 2D and s-IOT images indicate visible caries lesions. Arrows on the micro-CT indicate confirmed lesions. The tomosynthesis slices demonstrate increased lesion visibility, contrast and definition.

Image blur caused by patient and X-ray tube motion are common in tomosynthesis imaging owing to the relatively longer scan time than in 2D radiography. With the stationary X-ray source array, X-ray projections are acquired without any mechanical movement of the source. This reduces the time needed to move the source, as well as eliminating the source motion blur caused by translation of the X-ray tube. The acquisition time of a tomosynthesis using s-IOT is simply calculated as,

$$t_{total} = N \times \left(t_{exp} + t_{readout}\right) = \frac{D}{I_{tube}} + N \times t_{readout}$$

where N is the total number of projections, t_{exp} is the exposure time needed per projection, D is the total mAs of the tomosynthesis and t_{readout} is the image read-out time for each image. The first term D/I_{tube} gives the same total exposure time as 2D intraoral radiography since the same mAs and tube current are used, while the second term $N\ t_{\mathrm{readout}}$ is the extra time that s-IOT is needed for images to be extracted from the detector. At a given N, the acquisition time is mainly determined by the detector read-out speed. In this study, the SuniRay sensor was operated continuously at a speed of one frame per 5 s using a customized acquisition programme. The whole tomosynthesis acquisition took 75 s, which is too long for clinical applications. However, intraoral sensors capable of one frame per second are now technically feasible,[54] which will significantly reduce the total imaging time. The imaging time can be further shortened with faster sensors and smaller number of projections.

In this study, tomosynthesis images were acquired using the same dose as current 2D bitewing systems. Decreasing of the radiation dose may result in increased image noise. However, the TV regularization applied in the reconstruction reduces the image noises and artefacts, suggesting the potential for further reduction of the imaging dose, which will also shorten the imaging time.

The source array used in this s-IOT prototype was designed for other purposes with specifications different from those needed for dental imaging. To match the system resolution of current clinical intraoral devices, the system SID was increased. A CNT X-ray source array with smaller and isotropic focal spots has been fabricated.[33] This particular source array was operated at 5 mA tube current, comparable to the 7 mA tube current commonly used in intraoral imaging. The tube current of an X-ray tube, including the CNT source array, is mainly limited by the heat management of the anode.[42] For a focal spot size of 0.6×0.6 mm full width at half maximum, our prior thermal simulation shows that the anode can withstand 1.1 kW power, which

means that at 70 kVp, the source array can be operated at 15 mA tube current.

Conclusions

A proof-of-concept s-IOT system using a distributed CNT X-ray source array was constructed and evaluated. The system generated high-detail 3D information of the dental and alveolar anatomy with patient dose comparable to a standard 2D intraoral radiography. Phantom and extracted teeth phantom images show improved visibility and detection of dental pathologies such as caries, fractures and defects. The preliminary results obtained so far suggest that s-IOT using a CNT source array is a feasible technique that can potentially improve the diagnosis of caries detection, root fractures and other dental pathologies. The system has the potential to operate at a very low cost, low dose and in a time-efficient manner. The diagnostic efficacy of this modality will continue to be evaluated in more robust observer trials.

Conflicts of interest

The content is solely the responsibility of the authors and does not necessarily represent the official views of the NIH. Otto Zhou has equity ownership and serves on the board of directors of Xintek, Inc., to which the following technologies used or evaluated in this article have been or will be licensed: CNT X-ray source arrays and stationary intraoral tomosynthesis. Jianping Lu has equity ownership in Xintek, Inc. The authors of this article (JS, AWT, LRG, GTW, EP, AM, JPL and OZ) are inventors of a pending patent application on the stationary intraoral tomosynthesis technology.

References

1. Ruprecht A. Oral and maxillofacial radiology. *J Am Dent Assoc* 2008; **139**: S5–5. doi: 10.14219/jada.archive.2008.0355
2. Howerton WB Jr, Mora MA. Advancements in digital imaging: what is new and on the horizon? *J Am Dent Assoc* 2008; **139** (Suppl.): 20S–4S. doi: 10.14219/jada.archive.2008.0354
3. De Vos W, Casselman J, Swennen GR. Cone-beam computerized tomography (CBCT) imaging of the oral and maxillofacial region: a systematic review of the literature. *Int J Oral Maxillofac Surg* 2009; **38**: 609–25. doi: 10.1016/j.ijom.2009.02.028
4. Tyndall DA, Rathore S. Cone-beam CT diagnostic applications: caries, periodontal bone assessment, and endodontic applications. *Dent Clin North Am* 2008; **52**: 825–41. doi: 10.1016/j.cden.2008.05.002
5. Akdeniz BG, Gröndahl HG, Magnusson B. Accuracy of proximal caries depth measurements: comparison between limited cone beam computed tomography, storage phosphor and film radiography. *Caries Res* 2006; **40**: 202–7. doi: 10.1159/000092226
6. Tsuchida R, Araki K, Okano T. Evaluation of a limited cone-beam volumetric imaging system: comparison with film radiography in detecting incipient proximal caries. *Oral Surg Oral Med Oral Pathol Oral Radiol Endod* 2007; **104**: 412–16.
7. Nair MK, Tyndall DA, Ludlow JB, May K. Tuned aperture computed tomography and detection of recurrent caries. *Caries Res* 1998; **32**: 23–30. doi: 10.1159/000016426
8. Bader JD, Shugars DA, Bonito AJ. Systematic reviews of selected dental caries diagnostic and management methods. *J Dent Educ* 2001; **65**: 960–8.
9. Dove SB. Radiographic diagnosis of dental caries. *J Dent Educ* 2001; **65**: 985–90.
10. Li L, Chen Z, Zhao Z, Wu D. X-ray digital intra-oral tomosynthesis for quasi-three-dimensional imaging: system, reconstruction algorithm, and experiments. *Opt Eng* 2013; **52**: 013201.
11. Ziegler CM, Franetzki M, Denig T, Mühling J, Hassfeld S. Digital tomosynthesis-experiences with a new imaging device for the dental field. *Clin Oral Investig* 2003; **7**: 41–5. doi: 10.1007/s00784-003-0195-6
12. Cho MK, Kim HK, Youn H, Kim SS. A feasibility study of digital tomosynthesis for volumetric dental imaging. *J Instrumentation* 2012; **7**: P03007-P.
13. Franetzki M, Ploetz J, inventors. *X-ray diagnostic apparatus for tomosynthesis having a detector that detects positional relationships*. US Patent 5,828,722. 1998.
14. Webber RL, Horton RA, Tyndall DA, Ludlow JB. Tuned-aperture computed tomography (TACT). Theory and application for three-dimensional dento-alveolar imaging. *Dentomaxillofac Radiol* 1997; **26**: 53–62. doi: 10.1038/sj.dmfr.4600201
15. Harase Y, Araki K, Okano T. Diagnostic ability of extraoral tuned aperture computed tomography (TACT) for impacted third molars. *Oral Surg Oral Med Oral Pathol Oral Radiol Endod* 2005; **100**: 84–91. doi: 10.1016/j.tripleo.2004.12.001
16. Nair MK, Webber RL, Johnson MP. Comparative evaluation of tuned aperture computed tomography® for the detection of mandibular fractures. *Dentomaxillofac Radiol* 2000; **29**: 297–301. doi: 10.1038/sj.dmfr.4600548
17. Nair MK, Nair UP, Gröndahl HG, Webber RL. Accuracy of tuned aperture computed tomography in the diagnosis of radicular fractures in non-restored maxillary anterior teeth—an *in vitro* study. *Dentomaxillofac Radiol* 2002; **31**: 299–304. doi: 10.1038/sj.dmfr.4600712
18. Nair MK, Nair UDP, Gröndahl HG, Webber RL, Wallace JA. Detection of artificially induced vertical radicular fractures using tuned aperture computed tomography. *Eur J Oral Sci* 2001; **109**: 375–9.
19. Nair MK, Bezik J. Tuned-aperture computed tomography for detection of induced mid-buccal/lingual alveolar bone defects. *J Periodontol* 2006; **77**: 1833–8. doi: 10.1902/jop.2006.050452
20. Harase Y, Araki K, Okano T. Accuracy of extraoral tuned aperture computed tomography (TACT) for proximal caries detection. *Oral Surg Oral Med Oral Pathol Oral Radiol Endod* 2006; **101**: 791–6. doi: 10.1016/j.tripleo.2005.04.005
21. Nair MK, Tyndall DA, Ludlow JB, May K, Ye F. The effects of restorative material and location on the detection of simulated recurrent caries. A comparison of dental film, direct digital radiography and tuned aperture computed tomography. *Dentomaxillofac Radiol* 1998; **27**: 80–4. doi: 10.1038/sj.dmfr.4600323
22. Shi XQ, Han P, Welander U, Angmar-Månsson B. Tuned-aperture computed tomography for detection of occlusal caries. *Dentomaxillofac Radiol* 2001; **30**: 45–9. doi: 10.1038/sj/dmfr/4600576
23. Tingberg A. X-ray tomosynthesis: a review of its use for breast and chest imaging. *Radiat Prot Dosimetry* 2010; **139**: 100–7. doi: 10.1093/rpd/ncq099
24. Dobbins JT 3rd, McAdams HP. Chest tomosynthesis: technical principles and clinical update. *Eur J Radiol* 2009; **72**: 244–51. doi: 10.1016/j.ejrad.2009.05.054
25. Dobbins JT 3rd, McAdams HP, Godfrey DJ, Li CM. Digital tomosynthesis of the chest. *J Thorac Imaging* 2008; **23**: 86–92. doi: 10.1097/RTI.0b013e318173e162

26. Mermuys K, De Geeter F, Bacher K, Van De Moortele K, Coenegrachts K, Steyaert L, et al. Digital tomosynthesis in the detection of urolithiasis: diagnostic performance and dosimetry compared with digital radiography with MDCT as the reference standard. *AJR Am J Roentgenol* 2010; **195**: 161–7. doi: 10.2214/AJR.09.3075
27. Gomi T, Hirano H. Clinical potential of digital linear tomosynthesis imaging of total joint arthroplasty. *J Digit Imaging* 2008; **21**: 312–22. doi: 10.1007/s10278-007-9040-9
28. Geijer M, Börjesson AM, Göthlin JH. Clinical utility of tomosynthesis in suspected scaphoid fracture. A pilot study. *Skeletal Radiol* 2011; **40**: 863–7. doi: 10.1007/s00256-010-1049-3
29. Haas BM, Kalra V, Geisel J, Raghu M, Durand M, Philpotts LE. Comparison of tomosynthesis plus digital mammography and digital mammography alone for breast cancer screening. *Radiology* 2013; **269**: 694–700. doi: 10.1148/radiol.13130307
30. Zhang J, Yang G, Cheng Y, Gao B, Qiu Q, Lee YZ, et al. Stationary scanning x-ray source based on carbon nanotube field emitters. *Appl Phys Lett* 2005; **86**: 184104. doi: 10.1063/1.1923750
31. Zhou O, Calderon-Colon X. *Carbon nanotube and related field emitters: fundamentals and applications*. Weinheim, Germany: Wiley-VCH; 2010.
32. Qian X, Rajaram R, Calderon-Colon X, Yang G, Phan T, Lalush DS, et al. Design and characterization of a spatially distributed multibeam field emission x-ray source for stationary digital breast tomosynthesis. *Med Phys* 2009; **36**: 4389–99. doi: 10.1118/1.3213520
33. Qian X, Tucker A, Gidcumb E, Shan J, Yang G, Calderón-Colón X, et al. High resolution stationary digital breast tomosynthesis using distributed carbon nanotube X-ray source array. *Med Phys* 2012; **39**: 2090–9. doi: 10.1118/1.3694667
34. Tucker AW, Lu J, Zhou O. Dependency of image quality on system configuration parameters in a stationary digital breast tomosynthesis system. *Med Phys* 2013; **40**: 031917. doi: 10.1118/1.4792296
35. Shan J, Chtcheprov P, Tucker AW, Lee YZ, Wang X, Foos D, et al. Stationary chest tomosynthesis using a CNT X-ray source array. *Proc SPIE* 2013; **8668**: 86680E.
36. Shan J, Tucker AW, Lee YZ, Heath MD, Wang X, Foos DH, et al. Stationary chest tomosynthesis using a carbon nanotube X-ray source array: a feasibility study. *Phys Med Biol* 2015; **60**: 81–100. doi: 10.1088/0031-9155/60/1/81
37. Maltz JS, Sprenger F, Fuerst J, Paidi A, Fadler F, Bani-Hashemi AR. Fixed gantry tomosynthesis system for radiation therapy image guidance based on a multiple source X-ray tube with carbon nanotube cathodes. *Med Phys* 2009; **36**: 1624–36. doi: 10.1118/1.3110067
38. Gonzales B, Spronk D, Yuan C, Tucker AW, Beckman M, Zhou O, et al. Rectangular fixed-gantry CT prototype: combining CNT X-Ray sources and accelerated compressed sensing-based reconstruction. *IEEE* 2014; **2**: 971–81.
39. Abreu JM, Tyndall DA, Platin E, Ludlow JB, Phillips C. Two and three-dimensional imaging modalities for the detection of caries. A comparison between film, digital radiography and tuned aperture computed tomography (TACT). *Dentomaxillofac Radiol* 1999; **28**: 152–7. doi: 10.1038/sj.dmfr.4600430
40. *Performance standards for ionizing radiation emitting products*. 21 CFR 1020.30. Washington, DC: Food and Drug Administration; 2013.
41. Gomer R. *Field emission and field ionization*. Cambridge, MA: Harvard University Press; 1961.
42. Shan J, Zhou O, Lu J. Anode thermal analysis of high power micro-focus CNT X-ray tubes for *in-vivo* small animal imaging. *Proc SPIE* 2012; 83130. doi: 10.1117/12.911521
43. Marshall NW, Bosmans H. Measurements of system sharpness for two digital breast tomosynthesis systems. *Phys Med Biol* 2012; **57**: 7629–50. doi: 10.1088/0031-9155/57/22/7629
44. Wu G, Inscoe C, Calliste J, Lee YZ, Zhou O, Lu JP. Adapted fan-beam volume reconstruction for stationary digital breast tomosynthesis. *Proc SPIE* 2015; **9412**: 94123J.
45. Jensen TL, Jørgensen JH, Hansen PC, Jensen SH. Implementation of an optimal first-order method for strongly convex total variation regularization. *BIT Numer Math* 2012; **52**: 329–56. doi: 10.1007/s10543-011-0359-8
46. Soviero VM, Leal SC, Silva RC, Azevedo RB. Validity of MicroCT for *in vitro* detection of proximal carious lesions in primary molars. *J Dent* 2012; **40**: 35–40. doi: 10.1016/j.jdent.2011.09.002
47. Park YS, Bae KH, Chang J, Shon WJ. Theory of X-ray microcomputed tomography in dental research: application for the caries research. *J Korean Acad Conserv Dent* 2011; **36**: 98–107. doi: 10.5395/JKACD.2011.36.2.98
48. Brüllmann DD, Kempkes B, d'Hoedt B, Schulze R. Contrast curves of five different intraoral X-ray sensors: a technical note. *Oral Surg Oral Med Oral Pathol Oral Radiol* 2013; **115**: e55–61. doi: 10.1016/j.oooo.2013.03.007
49. Versteeg CH, Sanderink GC, van der Stelt PF. Efficacy of digital intra-oral radiography in clinical dentistry. *J Dent* 1997; **25**: 215–24. doi: 10.1016/S0300-5712(96)00026-7
50. Ludlow JB, Davies-Ludlow LE, White SC. Patient risk related to common dental radiographic examinations: the impact of 2007 International Commission on Radiological Protection recommendations regarding dose calculation. *J Am Dent Assoc* 2008; **139**: 1237–43. doi: 10.14219/jada.archive.2008.0339
51. Deller T, Jabri KN, Sabol JM, Ni X, Avinash G, Saunders R, et al. Effect of acquisition parameters on image quality in digital tomosynthesis. *Proc SPIE* 2007; **6510**: 65101L-L-11. doi: 10.1117/12.713777
52. Machida H, Yuhara T, Mori T, Ueno E, Moribe Y, Sabol JM. Optimizing parameters for flat-panel detector digital tomosynthesis. *Radiographics* 2010; **30**: 549–62. doi: 10.1148/rg.302095097
53. Shan J, Tucker AW, Lee YZ, Heath MD, Wang X, Foos D, et al. Evaluation of imaging geometry for stationary chest tomosynthesis. *Proc SPIE* 2014; **9033**: 903317. doi: 10.1117/12.2043314
54. Hamamatsu Photonics. CMOS area image sensors for X-ray imaging. [Updated 11 March 2013; cited 1 March 2015.] Available from: http://www.hamamatsu.com/jp/en/product/category/3100/4005/4126/S10830/index.html